Iranian Journal of Materials Science and Engineering, Vol. 21, Number 2, June 2024
RESEARCH PAPER

The Impact of Preparation Time on AgNPs Doped PVA and its Implication in Antimicrobial Activity

Wed A. Abed[1,*], Haider Abdulelah[2,*], Sanaa Q.Badr[2]

* *wed.abd@uobasrah.edu.iq & haider.abdulelah@uobasrah.edu.iq*

[1] Department of Pharmacognosy and Medicinal Plant, Pharmacy College, University of Basrah, Basrah, Iraq
[2] Department of Material Science, Polymer Research Centre, University of Basrah, Iraq

Received: March 2024 **Revised: May 2024** **Accepted: June 2024**
DOI: 10.22068/ijmse.3567

Abstract: *Silver/polyvinyl alcohol (Ag/PVA) nanocomposites were fabricated via an electrochemical method. Silver nanoparticles (AgNPs) with varying grain sizes were directly synthesized within PVA polymer matrices at deposition times of 15, 30, 45, 60, and 120 minutes. The integration of AgNPs within the PVA matrix was confirmed through Transmission Electron Microscopy (TEM) and optical absorbance measurements. X-ray Diffraction (XRD) analysis demonstrated the face-centered cubic structure of AgNPs. Furthermore, these prepared nanocomposites exhibited significant antibacterial properties against Bacillus subtilis and Pseudomonas pneumonia, as well as antifungal activity against Alternaria alternata. Remarkably, the AgNPs/PVA nanocomposite exhibited outstanding antifungal efficiency, resulting in an impressive inhibition zone of up to 47 mm.*

Keywords: *Ag/PVA nanocomposite, Electrochemical method, Antimicrobial activity.*

1. INTRODUCTION

A trend towards nanotechnology as one of the most rapidly advancing domains, with a notable emphasis on the synthesis and utilization of metal nanoparticles, positioning them as a paramount focal point of scholarly attention. Incorporating homogeneous dispersive metal nanoparticles into polymer host matrices plays a pivotal and multifaceted role in advancing numerous critical domains, encompassing optoelectronics, medicine, catalysis, water treatment, thermal stability, and biological sensing [1-3]. This integration facilitates significant progress and empowers innovative applications in each of these diverse fields [4, 5].
Besides silver (Ag), other metallic nanomaterials like copper, zinc, titanium [6], and gold [7] all show antibacterial activity, but silver has come up not only due to its highest antimicrobial activities but also due to some processing advantages like high-temperature stability and low volatility and to absorb and decompose ethylene [8, 9]. Among these transition metal elements, Ag stands out as particularly appealing due to its minimal human toxicity, broad spectrum of effects, and potent activity [10]. This can be attributed to their expanded surface area, which facilitates heightened interaction with microbial cells. The main limitation of this method is that the metal colloids coagulate, becoming unstable and problematic to use, as their antibacterial activities are reduced. One means of addressing this problem is to embed or surround the metal nanoparticles with polymer materials such as Polyvinyl alcohol (PVA), poly(vinylpyrrolidone) (PVP) and polystyrene (PS) [11, 12].
PVA represents a synthetic, non-toxic polymer renowned for its water-soluble nature. Its widespread adoption is attributed to its exceptional biocompatibility, thermo-stability, chemical resilience and biodegradability, rendering it invaluable across a spectrum of pragmatic applications [13, 14]. PVA's linear structural chains are enriched with a multitude of hydroxyl side groups, endowing it with notable reactivity and hydrophilic characteristics [15]. The exceptional attributes of PVA also extend to its application in hydrogel materials [16]. This is attributed to its distinctive medical properties, including a cooling sensation that aids in pain mitigation and the prevention of bacterial intrusion into the body. Additionally, PVA's capacity for bacteria entrapment is acknowledged [17]. Furthermore, the PVA matrix plays a pivotal role as a stabilizing agent, effectively curbing the aggregation of silver nanoparticles (AgNPs) filler [18, 19].
Many methods have been developed to prepare AgNPs; these include electrochemical, photochemical, microwave, gamma irradiation, and laser ablation techniques [20-22]. Although,

[DOI: 10.22068/ijmse.3567]

these techniques are problematic in terms of time, cost and complexity [12]. Electrochemical synthesis is most notable for its favorable attributes, including high production yield, simplicity, precise particle size control, elevated purity, and cost-effectiveness [12, 23]. However, there is an ongoing effort to develop a simpler method of incorporating silver in polymers.

Bacteria and fungi (Microorganisms) including Basillus sptillus, Pseudomonas pneumonia, and Alternaria alternata are commonly found in natural environments such as soil, water, and the gastrointestinal systems of both humans and animals [24]. In the realm of materials physics, AgNPs have garnered substantial attention for their remarkable ability to impede bacterial growth. The antibacterial mechanisms of AgNPs are multifaceted, encompassing: 1) Disruption of cell membranes, 2) Generation of reactive oxygen species (ROS), 3) Interaction with bacterial DNA, and 4) Inhibition of enzyme activity [25-28].

In this study, PVA emerges as a promising choice for composite formation, owing to its effective capping capabilities when integrated with AgNPs. Furthermore, the strategic integration of AgNPs into the PVA matrix through an electrochemical deposition process at various time intervals holds the potential to enhance the wound-healing attributes of the resulting hydrogel. This augmentation facilitates the maintenance of a moist environment, while concurrently serving as an effective antibacterial agent at the application site, thereby mitigating the risk of infections.

2. EXPERIMENTAL PROCEDURES

The Ag/PVA nanocomposite was synthesized using an electrochemical approach, which can be broken down into two key phases. In the first phase, a stabilizing agent, PVA with a molecular weight of 78,000 g/mol, was incorporated to forestall aggregation and ensure the isolation of particles. For this, 5 g of PVA was meticulously dissolved in 400 ml of deionized water (DW) under vigorous stirring at a temperature of 90°C. In the subsequent step, two polished bulk silver metal plates (commercially available, with a purity of 99.9%) were employed as cathode and anode working electrodes with a geometric area of (1.85 mm) diameter × (70 mm) length. The two were vertically positioned 5 cm apart, while submerged in 50 ml of PVA. A direct voltage (DC) source of 20 V was applied to the electrodes. The key variable in the synthesis was the reaction time, which was modulated across intervals of 15, 30, 45, 60, and 120 minutes to facilitate the dispersion of AgNPs within the polymer matrix. This process was carried out under controlled conditions and at room temperature (Fig. 1). The subsequent schematic elucidates the entirety of the experimental procedures.

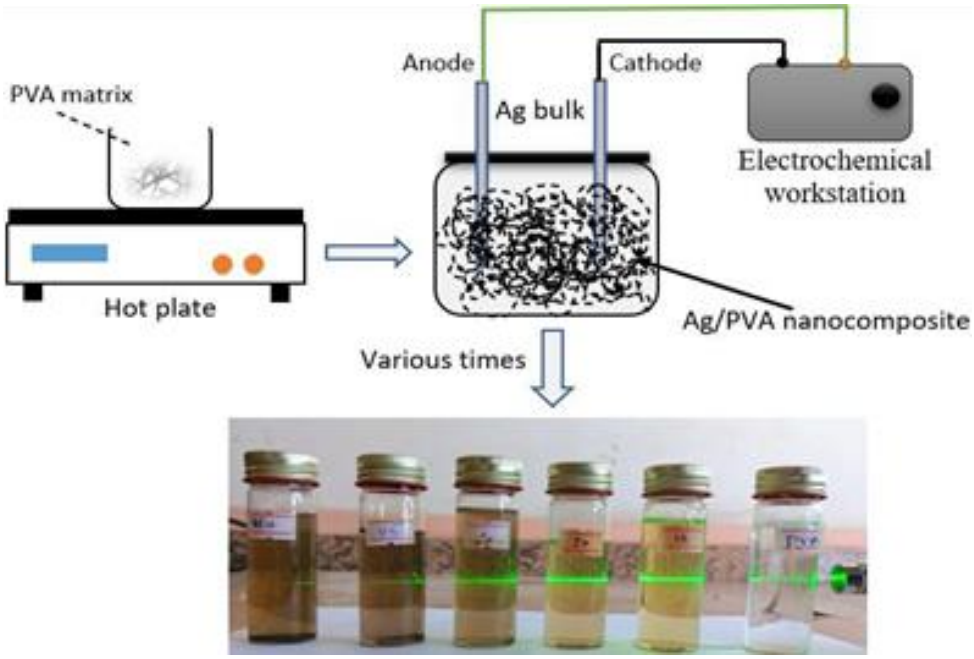

Fig. 1. Schematic form of Ag/PVA nanocomposite at various times.

[DOI: 10.22068/ijmse.3567]

The crystallographic properties of the synthesized Ag/PVA nanocomposites were comprehensively investigated utilizing X-ray diffraction (XRD) analysis. The experimental setup involved measuring angle 2θ values within the range of 20° to 80° using Cu Kα radiation, which possesses a wavelength of 1.5406 Å and was employed at grazing incidence (1 degree).

3. RESULTS AND DISCUSSION

3.1. XRD Analysis

The XRD diffraction patterns of both pristine PVA and Ag/PVA nanocomposites prepared at various time intervals are presented in Fig. 2.
A wide peak positioned at a 2θ angle of 19.6° in all three instances suggests the presence of the PVA semi-crystalline phase, specifically corresponding to the (110) reflection plane where the extended planer zig-zag chain direction of crystallites is found. This phenomenon is likely attributable to the strong intra-molecular hydrogen bonding within each monomer unit of PVA, as well as between different monomer units [29, 30].

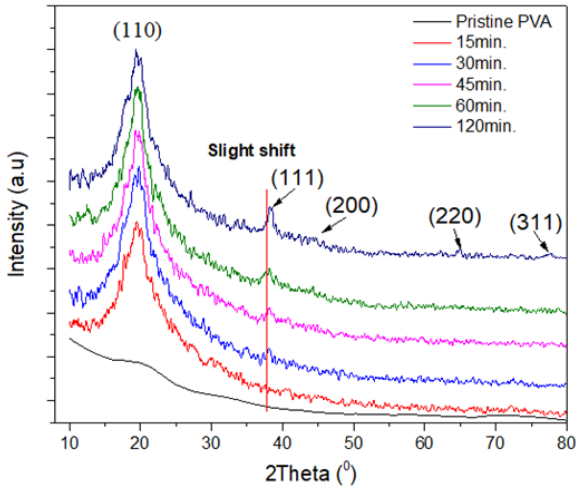

Fig. 2. XRD of PVA, and various samples of Ag/PVA nanocomposites.

The discernible peaks observed at 2θ positions of 38.4, 44.1, 64.7 and 77.6 in the XRD patterns correspond to the crystallographic planes within the Ag/PVA nanocomposites, specifically denoting (111), (200), (220), and (311) planes [31-33]. These crystalline facets signify the arrangement of nanoparticles within the PVA matrix and can be attributed to the face-centered cubic (FCC) phase of Ag NPs. Notably, the intensity of these diffraction peaks gradually increases with higher AgNPs concentrations. The most prominent peak, situated at 2θ= 38.40, corresponds to the (111) reflection plane and exhibits a slight angular shift, indicative of alterations in the corresponding d-spacing values.

3.2. TEM Analysis

Transmission electron microscopy (TEM) imaging was employed to investigate the morphology of Ag nanoparticles intricately associated with the PVA polymer's molecular chains in two distinct samples. These samples represent the extremes of concentration achieved through different preparation times namely, 15 minutes and 120 minutes. The TEM micrographs, depicted in Fig. 3, unveil an intricate interlacing structure indicative of AgNP-PVA interactions.
The TEM analysis reveals that the synthesized AgNPs exhibit a spherical morphology, characterized by remarkable homogeneity and smoothness, devoid of any observable aggregations. Notably, a diverse range of particle sizes is evident within each sample. After 15 minutes of preparation, AgNPs manifested as smaller entities with size distributions spanning the range of 10 to 20 nm, constituting the majority of the population (Fig. 3a). In contrast, as the preparation duration extended to 120 minutes, the concentration of AgNPs increased, prompting a discernible shift toward larger particle sizes, ultimately ranging from 40 to 50 nm (Fig. 3b).

3.3. Optical Analysis

The maximum typical band's spectrum appears limited between 350 to 540 nm in the visible region, It is a different value from the reported literature and coincides with the time when the comment starts to turn grey. However, as the time interval synthesis progresses, it can be observed that the colour changes from green-yellowish to dark grey as a result of an increase in grain size [17, 31, 34]. Fig. 4 reveals a gradual change in the maximum absorption band started at the first quartile minutes of formed AgNPs (418 nm) and increased during the reactions until reached 431 nm (Red shift) at 120 minutes and the crystallinity intensity increased caused by the surface plasmon band characteristics of silver as shown in Table 1. XRD patterns match with these results.

[DOI: 10.22068/ijmse.3567]

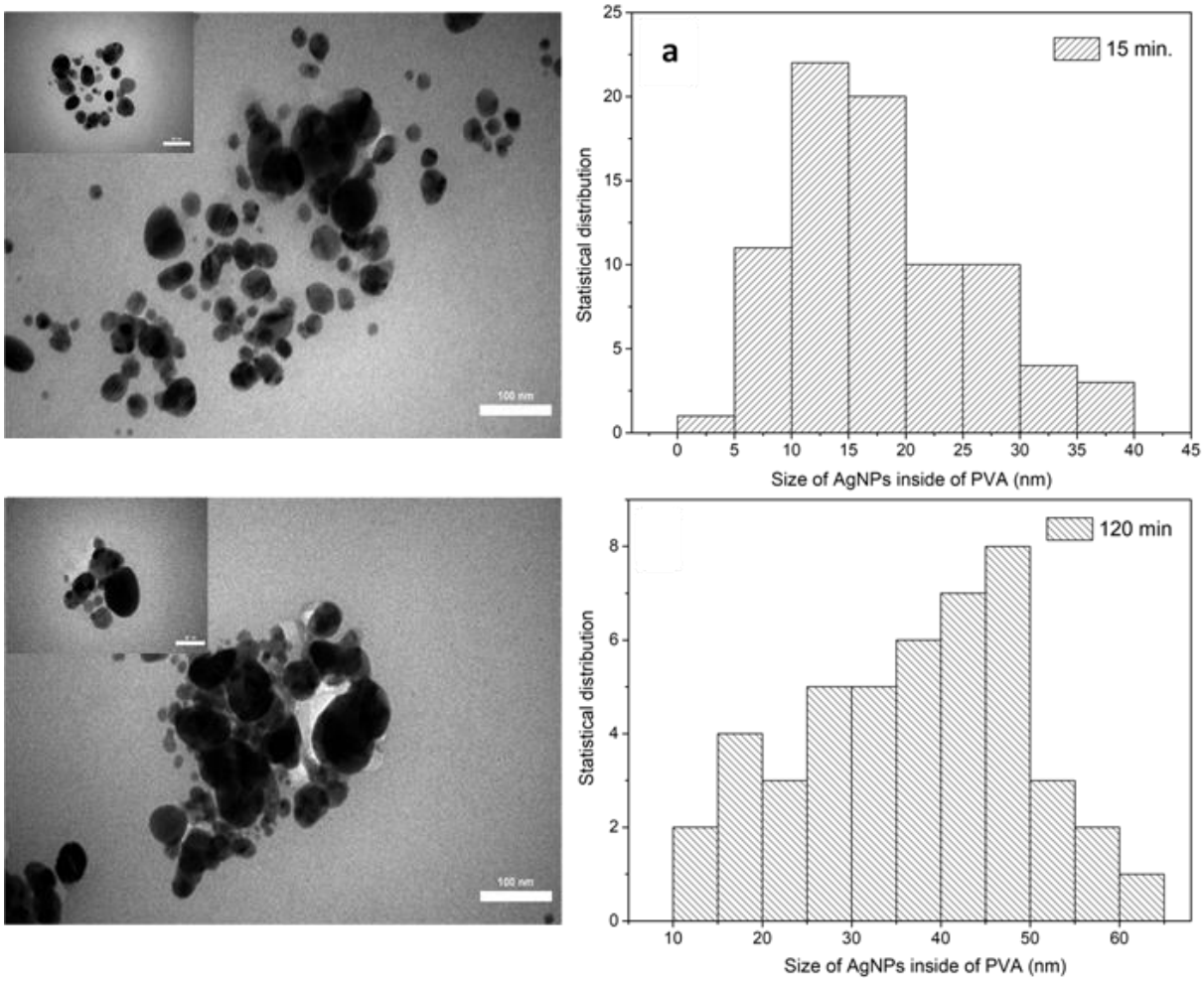

Fig. 3. TEM image and particle size of Ag nanoparticle generated inside of PVA. (a) 15 min., and, (b) 120 min.

The optical spectrum of the synthesized nanocomposites exhibits a prominent absorption band predominantly spanning the range of 350 to 540 nm within the visible region, representing a distinctive feature differing from prior literature reports. Notably, this spectral band coincides with the point at which the material undergoes a perceptible transition, transitioning from its initial green-yellowish hue to a deeper shade of dark grey. This transformation is a direct consequence of the progressive enlargement of grain size during the synthesis timeline. Fig. 4 offers compelling insights into this evolution of the maximum absorption band. Commencing at the initial quartile of the AgNP formation process (approximately 15 minutes), the maximum absorption band registers at 418 nm. As the synthesis proceeds, a notable redshift is observed, culminating at 431 nm after 120 minutes. This pronounced redshift is indicative of the increased crystallinity and is aligned with the surface plasmon band characteristics inherent to silver, as corroborated by the findings in Table 1. The agreement between these observations and the XRD patterns reinforces the consistency of these results.

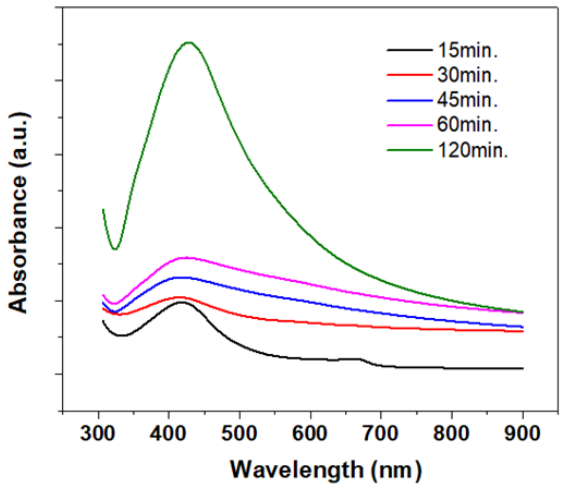

Fig. 4. Absorbance of AgNPs bonded to PVA matrix versus time preparation.

[DOI: 10.22068/ijmse.3567]

The optical characteristics outlined in this section illuminate the dynamic interplay between synthesis time, grain size evolution, and the resultant spectral attributes, underlining the precision control achievable in tailoring nanocomposite properties.

Table 1. Absorption maximum of Ag/PVA nanocomposite

Samples	Max. absorption (nm)
Ag/PVA (15 min.)	418
Ag/PVA (30 min.)	420
Ag/PVA (45 min.)	421
Ag/PVA (60 min.)	426
Ag/PVA (120 min.)	431

4. ANTIBACTERIAL/FUNGAL ACTIVITY

Bacterial and fungal cultures were cultivated on nutrient and potato dextrose agar at 37°C for 24 hours. Circular voids with a 3 cm diameter were created within the agar-containing petri dishes. The antibacterial efficacy of AgNPs (varying preparation times)/PVA polymer was assessed against Basillus sptillus and Pseudomonus pneumonia bacteria, as depicted in Fig. 5 and 6. Notably, pristine PVA exhibited no inherent antibacterial properties, necessitating the incorporation of AgNPs into the PVA matrix. Remarkably, within the inhibition zone, exposure to the Ag/PVA composite led to the complete elimination of bacterial cells. Specifically, the 15 minute sample targeting P. pneumonia demonstrated a substantial inhibition zone with a diameter of 3.3 cm. Furthermore, an increase in Ag particle size within the PVA matrix corresponded to an expanded inhibition zone, culminating at 4.2 cm, in contrast to B, sptillus bacteria which exhibited a 4 cm inhibition zone. Previous research by G.Y. Nigussie et al. [35] elucidated that the increased average AgNP diameter with time delays recombination and augments antibacterial activity.

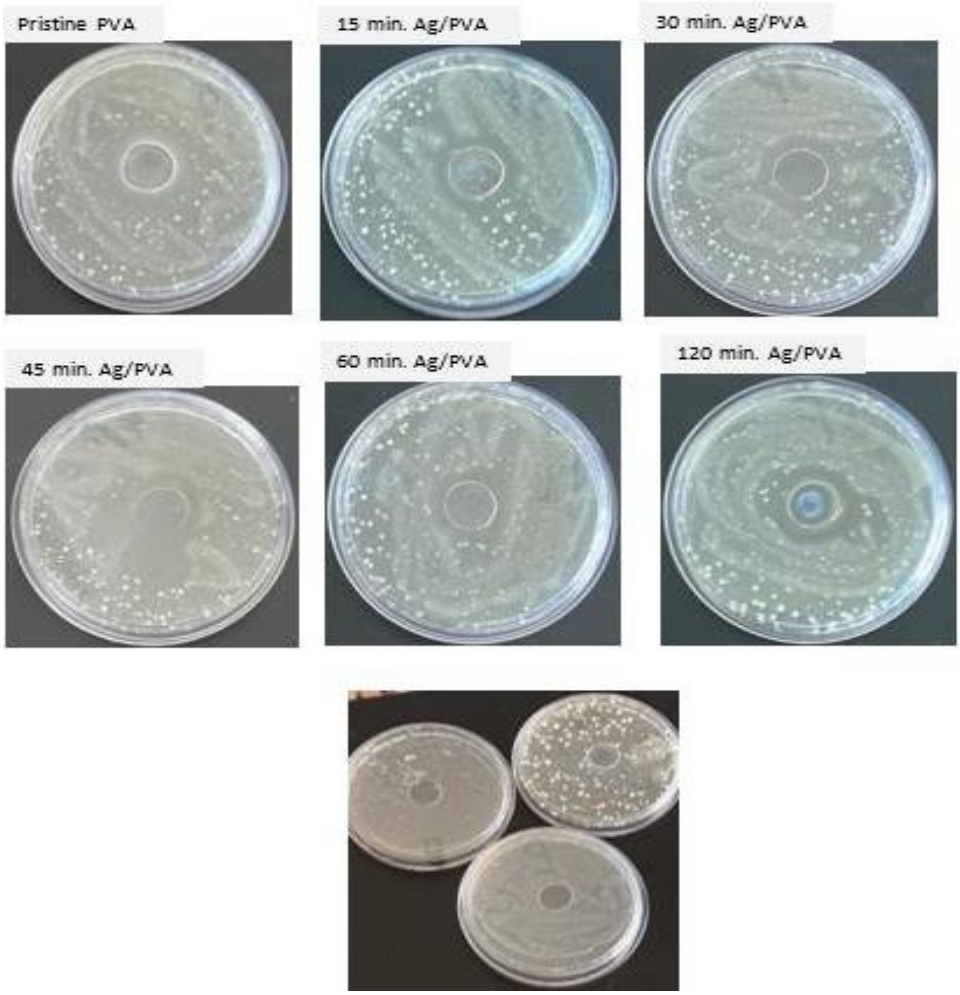

Fig. 5. Antibacterial activity images of Ag/PVA against Pseudomonus pneumonia, and controller.

[DOI: 10.22068/ijmse.3567]

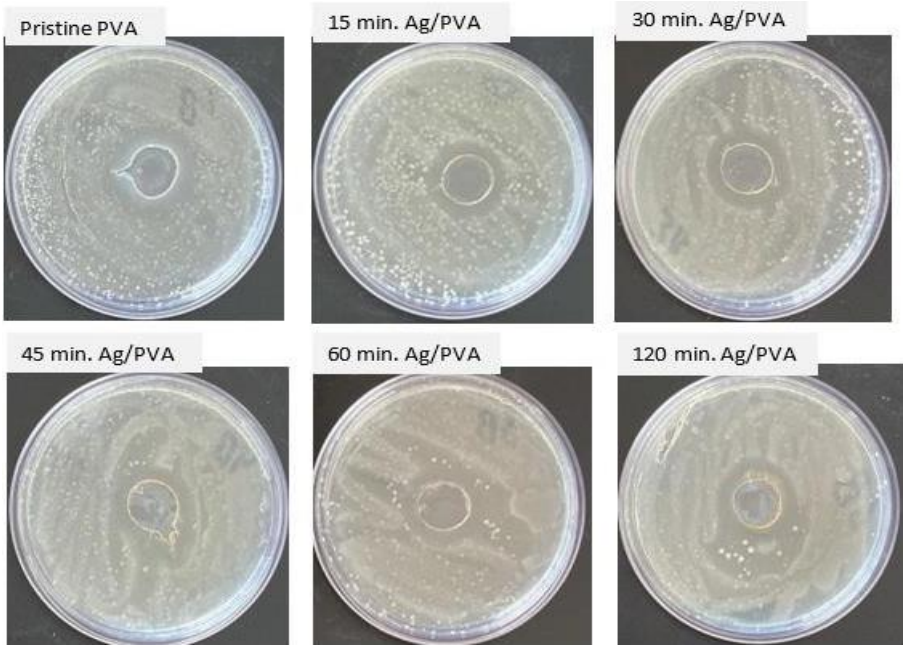

Fig. 6. Antibacterial activity images of Ag/PVA against Basillus sptillus

Fig. 7 illustrates the antifungal activities against alternata, initiating at lower concentrations and smaller Ag/PVA particle sizes, denoted as the '15min.' sample (37 mm). However, this activity escalated as the particle size increased, ultimately reaching 45 mm after 120 minutes. This substantial disruption of fungal cell function culminated in cell death, contrasting the antibacterial effect. The underlying reason for this phenomenon may be attributed to the intricate and fortified cell wall composition of fungi, featuring chitin, glucans, and various polysaccharides. Silver nanoparticles exhibit heightened efficacy in disrupting fungal cell walls, surpassing their impact on bacterial cell walls primarily composed of peptidoglycan. The structural differences between these cell walls make fungi are vulnerable to damage by Ag nanoparticles. All details are explained in the following Table 2.

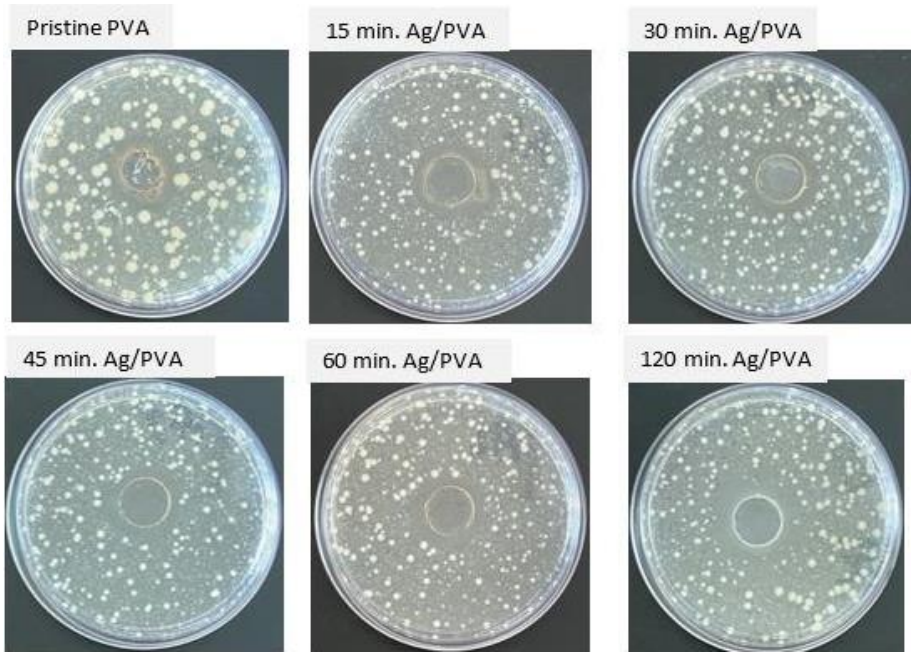

Fig. 7. Antifungal activity images of Ag/PVA against Alternaia alternata

[DOI: 10.22068/ijmse.3567]

Table 2. Diameter of inhibition zone (mm)

Samples	Basillus sptillus	Pseudomonus pneumonia	Alternaia alternata
Pristine PVA	….	….	….
Ag/PVA (15 min.)	31	33	37
Ag/PVA (30 min.)	33	35	41
Ag/PVA (45 min.)	33	37	43
Ag/PVA (60 min.)	36	39	45
Ag/PVA (120 min.)	40	42	47

5. CONCLUSIONS

This study successfully synthesized noble metal AgNPs doped within a PVA polymer matrix via the electrochemical method. The controlled experiment duration led to the modulation of grain sizes, resulting in a distinct shift in coloration from greenish to grey, indicative of a redshift phenomenon. The Ag/PVA nanocomposites exhibited promising antibacterial properties against common infection-causing microorganisms, including Basillus sptillus and Pseudomonus pneumonia. Furthermore, they demonstrated efficacy in countering Alternaia alternata fungus, a pathogen associated with respiratory infections and asthma. Notably, the Ag/PVA nanocomposites synthesized over 120 minutes exhibited the highest inhibitory zone diameter, reaching an impressive 47 mm.

REFERENCES

[1]. Nimrodh Ananth, A., Umapathy, S., Sophia, J., Mathavan, T., Mangalaraj, D., "On the optical and thermal properties of in situ/ex situ reduced Ag NP's/PVA composites and its role as a simple SPR-based protein sensor." Appl. Nanosci., 2011, 1, 87-96.

[2]. Wang, P.-H., Wu, Y.-Z., Zhu, Q.-R., "Polymer metal composite particles: polymer core and metal shell." J. Mater. Sci., 2002, 21, 1825-1828.

[3]. Clémenson, S., Alcouffe, P., David, L., Espuche, E., "Structure and morphology of membranes prepared from polyvinyl alcohol and silver nitrate: influence of the annealing treatment and the film thickness." Desalination, 2006, 200, 437-439.

[4]. Pandey, S., Pandey, S. K., Parashar, V., Mehrotra, G., Pandey, A. C., "Ag/PVA nanocomposites: optical and thermal dimensions." J. Mater. Chem., 2011, 21, 17154-17159.

[5]. Solov'ev, A. Y., Potekhina, T., Chernova, I., Basin, B. Y., "Track membrane with immobilized colloid silver particles." Russ. J. Appl. Chem., 2007, 80, 438-442.

[6]. Schabes-Retchkiman, P., Canizal, G., Herrera-Becerra, R., Zorrilla, C., Liu, H., Ascencio, J., "Biosynthesis and characterization of Ti/Ni bimetallic nanoparticles." Opt. Mater., 2006, 29, 95-99.

[7]. Won, H. I., Nersisyan, H., Won, C. W., Lee, J.-M., Hwang, J.-S., "Preparation of porous silver particles using ammonium formate and its formation mechanism." J. Chem. Eng., 2010, 156, 459-464.

[8]. Naskar, A., Kim, K. S., "Recent Advances in Nanomaterial-Based Wound-Healing Therapeutics." Pharmaceutics, 2020, 12, 499.

[9]. Frei, A., Verderosa, A. D., Elliott, A. G., Zuegg, J., Blaskovich, M. A. T., "Metals to combat antimicrobial resistance." Nat. Rev. Chem., 2023, 7, 202-224.

[10]. Almatroudi, A., "Silver nanoparticles: synthesis, characterisation and biomedical applications." Open Life Sci, 2020, 15, 819-839.

[11]. Krzywicka, A., Megiel, E., "Silver-Polystyrene (Ag/PS) Nanocomposites Doped with Polyvinyl Alcohol (PVA)-Fabrication and Bactericidal Activity." Nanomaterials (Basel), 2020, 10, 2245.

[12]. Bo, L., Yang, W., Xue, Q., Gao, J., "Antibacterial properties of silver/ polyvinyl alcohol colloids." Chem Org, 2007, 9, 52.

[13]. Han, M., Yun, J., Kim, H.-I., Lee, Y.-S., "Effect of surface modification of graphene oxide on photochemical stability of poly (vinyl alcohol)/graphene oxide composites." J. Ind. Eng. Chem., 2012, 18, 752-756.

[DOI: 10.22068/ijmse.3567]

[14]. Batool, S., Hussain, Z., Niazi, M. B. K., Liaqat, U., Afzal, M., "Biogenic synthesis of silver nanoparticles and evaluation of physical and antimicrobial properties of Ag/PVA/starch nanocomposites hydrogel membranes for wound dressing application." J. Drug Deliv. Technol., 2019, 52, 403-414.
[15]. Gaume, J., Rivaton, A., Thérias, S., Gardette, J.-L., "Influence of nanoclays on the photochemical behaviour of poly(vinyl alcohol)." Polym. Degrad. Stab., 2012, 97, 488-495.
[16]. Wang, M., Bai, J., Shao, K., Tang, W., Zhao, X., Lin, D., Huang, S., Chen, C., Ding, Z., Ye, J., "Poly (vinyl alcohol) hydrogels: The old and new functional materials." Int. J. Polym. Sci., 2021, 2021, 1-16.
[17]. Swaroop, K., Francis, S., Somashekarappa, H., "Gamma irradiation synthesis of Ag/PVA hydrogels and its antibacterial activity." Mater. Today Proc., 2016, 3, 1792-1798.
[18]. Surudžić, R. D., Jovanović, Ž., Bibić, N. M., Nikolić, B. Ž., Mišković-Stanković, V. B., "Electrochemical synthesis of silver nanoparticles in poly (vinyl alcohol) solution." J. Serb. Chem. Soc., 2013, 78, 2087-2098.
[19]. Xu, L., Wang, Y. Y., Huang, J., Chen, C. Y., Wang, Z. X., Xie, H., "Silver nanoparticles: Synthesis, medical applications and biosafety." Theranostics, 2020, 10, 8996-9031.
[20]. Long, D., Wu, G., Chen, S., "Preparation of oligochitosan stabilized silver nanoparticles by gamma irradiation." Radiat. Phys. Chem., 2007, 76, 1126-1131.
[21]. Mallick, K., Witcomb, M., Scurrell, M., "Polymer stabilized silver nanoparticles: a photochemical synthesis route." J. Mater. Sci., 2004, 39, 4459-4463.
[22]. Yin, H., Yamamoto, T., Wada, Y., Yanagida, S., "Large-scale and size-controlled synthesis of silver nanoparticles under microwave irradiation." Mater. Chem. Phys., 2004, 83, 66-70.
[23]. Reetz, M. T., Winter, M., Breinbauer, R., Thurn-Albrecht, T., Vogel, W., "Size-Selective Electrochemical Preparation of Surfactant-Stabilized Pd-, Ni-and Pt/Pd Colloids." Chem. Eur. J., 2001, 7, 1084-1094.
[24]. Melo-Nascimento, A. O. d. S., Treumann, C., Neves, C., Andrade, E., Andrade, A. C., Edwards, R., Dinsdale, E., Bruce, T., "Functional characterization of ligninolytic Klebsiella spp. strains associated with soil and freshwater." Arch. Microbiol., 2018, 200, 1267-1278.
[25]. Feng, Q. L., Wu, J., Chen, G. Q., Cui, F., Kim, T., Kim, J., "A mechanistic study of the antibacterial effect of silver ions on Escherichia coli and Staphylococcus aureus." J. Biomed. Mater. Res., 2000, 52, 662-668.
[26]. Kim, S.-H., Lee, H.-S., Ryu, D.-S., Choi, S.-J., Lee, D.-S., "Antibacterial activity of silver-nanoparticles against Staphylococcus aureus and Escherichia coli." Korean J. Microbiol. Biotechnol, 2011, 39, 77-85.
[27]. Girase, B., Depan, D., Shah, J., Xu, W., Misra, R., "Silver–clay nanohybrid structure for effective and diffusion-controlled antimicrobial activity." Mater. Sci. Eng. C., 2011, 31, 1759-1766.
[28]. Li, Q., Mahendra, S., Lyon, D. Y., Brunet, L., Liga, M. V., Li, D., Alvarez, P. J., "Antimicrobial nanomaterials for water disinfection and microbial control: potential applications and implications." Water Res, 2008, 42, 4591-4602.
[29]. Strawhecker, K., Manias, E., "Structure and properties of poly (vinyl alcohol)/Na^+ montmorillonite nanocomposites." Chem. Mater., 2000, 12, 2943-2949.
[30]. Bogle, K., Dhole, S., Bhoraskar, V., "Diffusion mediated growth of (111) oriented silver nanoparticles in polyvinyl alcohol film under 6MeV electron irradiation." Appl. Phys. Lett., 2006, 88, 3105.
[31]. Ghanipour, M., Dorranian, D., "Effect of Ag-nanoparticles doped in polyvinyl alcohol on the structural and optical properties of PVA films." J. Nanomater., 2013, 2013, 1.
[32]. Saini, I., Rozra, J., Chandak, N., Aggarwal, S., Sharma, P. K., Sharma, A., "Tailoring of electrical, optical and structural properties of PVA by addition of Ag nanoparticles." Mater. Chem. Phys., 2013,

[DOI: 10.22068/ijmse.3567]

139, 802-810.
[33]. Mahendia, S., Tomar, A., Kumar, S., "Nano-Ag doping induced changes in optical and electrical behaviour of PVA films." Mater. Sci. Eng. B, 2011, 176, 530-534.
[34]. Asif, M., Yasmin, R., Asif, R., Ambreen, A., Mustafa, M., Umbreen, S., "Green synthesis of silver nanoparticles (AgNPs), structural characterization, and their antibacterial potential." Dose-Response, 2022, 20, 15593258221088709.
[35]. Nigussie, G. Y., Tesfamariam, G. M., Tegegne, B. M., Weldemichel, Y. A., Gebreab, T. W., Gebrehiwot, D. G., Gebremichel, G. E., "Antibacterial activity of Ag-doped TiO_2 and Ag-doped ZnO nanoparticles." Int. J. Photoenergy, 2018, 1, 1–7.

[DOI: 10.22068/ijmse.3567]